Teresa Mikolajczyk,
***Stanisław Rabiej,**
Grzegorz Szparaga,
Maciej Boguń,
****Aneta Fraczek-Szczypta,**
****Stanisław Błażewicz**

Technical University of Łódź,
Department of Man-Made Fibres,
Faculty of Material Technologies
and Textile Design
ul. Żeromskiego 116, 90-924 Łódź, Poland
E-mail: mikolter@p.lodz.pl

***Department of Materials**
and Environmental Sciences,
University of Bielsko-Biala,
ul. Willowa 2, 43-309 Bielsko-Biala, Poland

****Department of Biomaterials,**
Faculty of Materials Science and Ceramics,
AGH- University of Science and Technology,
Al. Mickiewicza 30, 30-059 Kraków, Poland

Strength Properties of Polyacrylonitrile (PAN) Fibres Modified with Carbon Nanotubes with Respect to Their Porous and Supramolecular Structure

Abstract
This work was dedicated to the investigation of the influence of the effect of carbon nanotubes on the porous and supramolecular structure of precursor polyacrylonitrile (PAN) fibres. A relationship was found between the structure of the fibers produced in a two-stage and three-stage drawing process and the strength properties of those fibres. The structural parameters and properties of PAN fibres modified with carbon nanotubes were compared with corresponding values for the fibres without nanoadditives. It was found that the introduction of carbon nanotubes into the material of PAN fibres increases their deformability at successive stages of drawing to a degree depending on the type of nanotube. This was the main reason for their higher strength properties in comparison with the fibres without a nanoadditive.

Key words: *carbon nanotubes, nanocomposites, fibres, porous structure, WAXS.*

Introduction

Polyacrylonitrile (PAN) fibres are a basic precursor for obtaining carbon fibres. Carbon fibres with new properties are obtained not only by modification of the structure of the precursor fibres [1 – 3], but also by the introduction of various types of nanoadditives, including carbon nanotubes [4 – 11]. Carbon nanotubes have a number of advantageous properties which cause them to be used for the modification of polymers. With high theoretical strength and Young's modulus, they display high elasticity and a susceptibility to stretching, twisting and bending. Single-walled nanotubes are more prone to stretching, while the multi-walled variety are more effective at transferring compressive stresses. This results from the mutual slipping of the cylindrical graphene layers of which multi-walled nanotubes are built [12 – 17].

Depending on their type (MWNT or SWNT), nanotubes differ in their electrical and magnetic properties. They also display interesting thermal properties [14].

These features mean that the modification of PAN fibres with carbon nanotubes produces specific properties of carbon fibres obtained from this precursor. The presence of nanotubes in the material of PAN fibres also ought to have an effect on the mechanism of their solidification and on deformation processes. We identified such effects for ceramic nanoadditives [18], ferromagnetic nanoadditives [19, 20] and nanosilver [21].

A work related to the production of PAN fibres containing carbon nanotubes [9] shows that the introduction of such tubes into the material of the fibres causes increased strength properties in comparison with fibres without nanotubes. This is accompanied by a decrease in the degree of crystallinity and a change in the size of the crystallites of the fibres. These fibres (containing various types of nanotubes) have been formed using a dry-wet method [9] or gel method [11], generally with a constant volume of deformation in drawing stage of the process. However, our investigations [22] were dedicated to the production of fibres with nanotubes (SWNT and MWNT) using deformations close to the maximum (achievable for fibres with a given type of nanotubes). This method facilitated exploitation of the potential capabilities of the material and determination of the influence of the presence of various types of nanotubes on the deformation processes. Moreover, the forming process was carried out with a positive value of the as-spun draw ratio. This favoured the orientation of structural elements in the still liquid stream and the production of fibres with a diameter of

Table 1. *Characterisation of nanotubes.*

Type of nanotubes	Length, nm	Diameter, nm	Internal surface, m^2/g	Producer
MWNT-A – multiwalled carbon nanotubes	300-2000	5-20	20	Nanocraft, modified in AGH Cracow
SWNT – single wall carbon nanotubes	30-50	2-3	220	Nanocraft
MWNT-S – multiwalled carbon nanotubes	1000-2000	10-30	40-600	Nanostructured & Amorphus Materiale Inc.
MWNT-L – multiwalled carbon nanotubes	10000-30000	10-20	200-350	Nanostructured & Amorphus Materiale Inc.

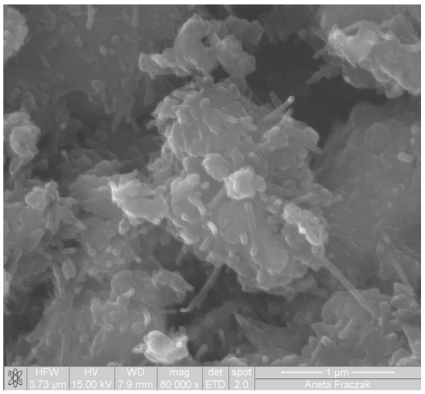

Figure 1. *NanoSEM microscope image of MWNT-A.*

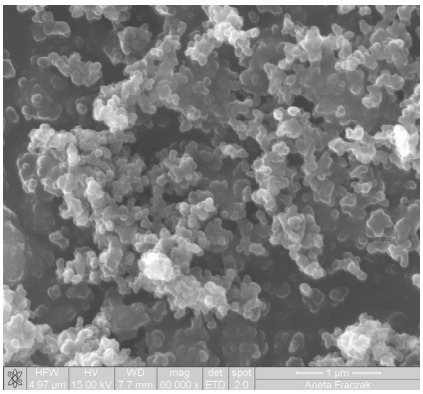

Figure 2. *NanoSEM microscope image of SWNT.*

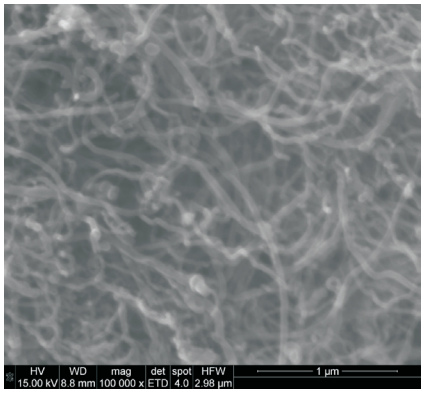

Figure 3. *NanoSEM microscope image of MWNT-S.*

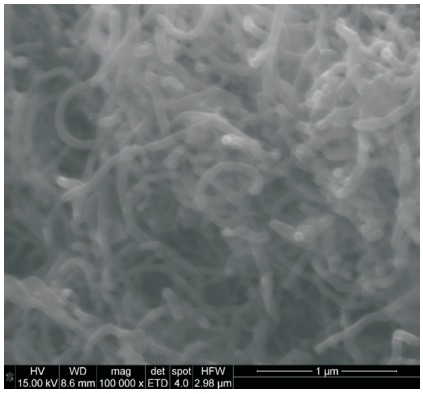

Figure 4. *NanoSEM microscope image of MWNT-L.*

approximately 10 µm. The use of a three-stage drawing process, with a suitable distribution of deformation at different stages, favoured the production of fibres with increased strength properties [22]. This also prevents the effect of over-stretching precursor fibres, as identified by us [23], which may have a negative effect on the properties of carbon fibres. In this work an attempt was made to clarify the cause of differences in the tensile properties of precursor fibres containing different types of carbon nanotubes. The basis of this investigation was analysis of the porous and supramolecular structure of such fibres. Also the influence of dividing the process of drawing into stages on changes in the structure and changes in the tensile properties of the fibres resulting from it were included. It is also significant that, in contrast to the research described in the literature [9 – 11], the subject of our work is a multifilament rather than a monofilament, which widens the scope of the research to include findings on important areas of application.

The aim of this work was to make a comparative analysis of the strength properties of polyacrylonitrile fibres modified with various types of carbon nanotubes in terms of their porous and supramolecular structure.

Materials and methods

A spinning solution was prepared from polyacrylonitrile copolymer (PAN), manufactured by Zoltek, with an intrinsic viscosity of 1.46 dl/g (determined in DMF at a temperature of 20 °C).

The average weight and number of molecular masses, determined by GPC, using DMAc as a solvent with the addition of 0.5% lithium chloride, amounted to Mw = 249930 and Mn = 92577, the polydispersity index being 2.7.

Four types of carbon nanotubes were used, the characteristics of which are given in ***Table 1***. Photographs of the carbon nanotubes used in the work, taken with a NanoSEM microscope (Nova NanoSEM 200, FEI), are shown in ***Figures 1 – 4***. Rheological properties of the spinning solutions and the values of the rheological parameters with their interpretation are described in [22].

Fibre formation

Fibres were formed from wet solution using a large laboratory spinning machine. The spinning solutions used were 23.5% solutions of polyacrylonitrile in DMF containing 1% of carbon nanotubes in proportion to the polymer. The spinning solution was prepared by obtaining a homogeneous suspension of carbon nanotubes in DMF, and then introducing a polymer into it. The process of preparation of a suspension of nanotubes in the solvent involved the homogenisation of the mixture of nanotubes in DMF using a Bandelin Sonopuls HD 2200 ultrasound homogeniser. The process was carried out at a temperature of 20 °C for 30 minutes.

The fibres were spun with a large laboratory spinning machine whose design enables the technological parameters to be stabilised, constantly monitored, and varied over a wide range.

A 500-hole spinning nozzle was used, with holes of 0.08 mm in diameter.

Solidification of the fibres took place in water baths containing 60% DMF at a temperature of 20 °C. The fibres were formed with a positive value of the as-spun draw ratio of +75%.

Two variants of the fibre drawing process were applied: a two-stage process and a three-stage process. In the two-stage variant, the first stage of drawing took place in a plastifying water bath containing 50% DMF at a temperature of 70 °C, with a deformation of 0.7 of its maximum value. The second stage of drawing was carried out in superheated steam at a temperature of 135 °C with maximum deformation achievable. After the drawing process the fibres were rinsed and dried in isometric conditions at a temperature of 20 °C.

In the three-stage version of the drawing process, the first stage was the same as in the first variant, but at the second stage a deformation of 0.9 of the maximum value was used. After the second drawing stage the fibres were rinsed in order to remove the residual solvent, dried and then subjected to a further stage of drawing in an atmosphere of superheated steam at a temperature of 165 °C. This drawing stage was carried out at the maximum deformation value achievable.

Table 2. *Spinning conditions and properties of PAN fibres modified with various types of nanotubes, subjected to a two-stage drawing process.*

Sample symbol	Type of nanotubes	Total deformation	Fibres diameter, μm	Young's modulus, GPa	Tenacity, MPa	Elongation at break, %	Total volume of pores, cm^3/g	Volume of pores in the range 3 - 1000 nm, cm^3/g	Total internal surface, m^2/g	Crystallinity, %	L_{110}, Å	d_{110}, Å
SR 3	MWNT-A	17.76	10.4 ± 0.31	10.3 ± 0.31	570 ± 17	12.71 ± 0.38	0.461	0.150	29.010	57	50	5.3
SR 5	SWNT	18.17	9.9 ± 0.30	10.3 ± 0.31	560 ± 17	11.70 ± 0.35	0.448	0.232	52.217	55	41	5.4
SR 7	MWNT-L	19.52	9.3 ± 0.28	8.6 ± 0.26	540 ± 16	11.37 ± 0.34	0.404	0.148	19.287	53	48	5.3
SR 9	MWNT-S	19.60	8.9 ± 0.27	10.4 ± 0.31	570 ± 17	11.87 ± 0.36	0.452	0.172	31.729	68	48	5.4
SN 13	-------	18.46	9.7 ± 0.29	7.8 ± 0.23	510 ± 15	12.84 ± 0.38	0.461	0.135	20.390	55	46	5.4

Table 3. *Spinning conditions and properties of PAN fibres modified with various types of nanotubes, subjected to a three-stage drawing process.*

Sample symbol	Type of nanotubes	Total deformation	Fibres diameter, μm	Young's modulus, GPa	Tenacity, MPa	Elongation at break, %	Total volume of pores, cm^3/g	Volume of pores in the range 3-1000 nm, cm^3/g	Total internal surface, m^2/g	Crystallinity, %	L_{110}, Å	d_{110}, Å
SR 3/1	MWNT-A	20.79	9.8 ± 0.29	12.1 ± 0.31	570 ± 17	8.36 ± 0.25	0.469	0.278	61.53	56	74	5.3
SR 5/2	SWNT	21.15	9.6 ± 0.29	11.5 ± 0.34	540 ± 16	8.22 ± 0.25	0.548	0.244	57.542	46	72	5.3
SR7/1	MWNT-L	23.47	9.0 ± 0.27	12.2 ± 0.36	620 ± 19	8.22 ± 0.25	0.496	0.242	50.685	43	75	5.3
SR 9/1	MWNT-S	21.50	8.8 ± 0.26	11.0 ± 0.33	630 ± 19	8.53 ± 0.26	0.384	0.120	18.527	50	72	5.4
SN 13/1	-------	18.56	9.2 ± 0.28	9.5 ± 0.28	530 ± 16	9.18 ± 0.27	0.652	0.304	57.18	62	73	5.4

This procedure was chosen because, according to our work [24], the strength properties of fibres are determined not only by the value of the total draw ratio but also by the distribution of deformation values at particular stages of the process. To obtain fibres with increased strength properties, it is advantageous to carry out a multi-stage drawing process in media with an increasing temperature.

The breaking force of elementary fibres was measured using a Zwick strength-testing machine, model 1435. The tenacity was computed from the tearing force based on the cross-sectional area of the fibres, which was calculated from the diameter of the fibres, assuming them to be circular.

The porosity of the fibres was determined by the mercury porosimetry method, using a Carlo-Erba porosimeter coupled to a computer system, which enabled determination of the total volume of pores, the size distribution of pores in the size range 3 – 7500 nm, and the total internal surface of the pores.
Photos of fiber cross-sections were taken with a JEOL JSM-5200LV scanning electron microscope. The cross-section preparations were examined by the low-pressure technique with the use of a detector of backscattered electrons (the pressure in the sample chamber was within the range of 6 Pa to 270 Pa). Observation was carried out at an accelerating voltage of 25 kV and magnification of 2000× and 5000×. Images were recorded by a Semafor digital system.

The crystalline structure was investigated using a URD 6 diffractometer from Seifert (Germany), operated at U = 40 kV and I = 30 mA, with a copper target X-ray tube. CuKα radiation of wavelength λ =1.54 Å was mochromatised using a graphite monochromator. Diffraction curves were recorded using the symmetrical reflection method and step measurement mode. The angular range recorded was 2θ = 6° to 60°, with a step size of 0.1°. An important stage of the preparation of samples was the powdering of the fibres using a microtome in order to eliminate texture, followed by pressing into tablets approximately 2 cm in diameter, with a thickness of 1 mm.

Analysis of the diffraction curves (WAXS) and calculations of degree of crystallinity were performed using a WAXSFIT computer program [25]. At the first stage a linear background was subtracted from the curves, determined based on the level of radiation intensity at small and large scatter angles. The diffractograms were also normalised to a uniform level of integral radiation intensity over the entire measurement range. Next the experimental diffraction curve was approximated by a theoretical curve, being the sum of functions representing individual crystalline peaks and an amorphous component. The curve-fitting procedure was carried out using a multi-criterion optimisation procedure and a hybrid system combining a genetic algorithm with Powell's classical optimisation method [26].

In this procedure, both the crystalline peaks and the amorphous maxima were represented by a function which is a linear combination of the Gauss and Lorentz functions. The initial angular positions of the crystalline peaks and the corresponding Miller indices were found based on the parameters of the PAN unit cell, as determined by Stefani [27, 28]. According to Stefani, the unit cell of PAN is orthorhombic, with the lengths of edges being a = 10.2 Å, b = 6.1 Å, and c = 5.1 Å. The amorphous component was approximated using two wide maxima, one of which is located at the scattering angle 2θ ≈ 24°, and the other at 2θ ≈ 36°.

The degree of crystallinity was calculated as the ratio of the integral intensity contained within the crystalline peaks to the integral intensity of the radiation scattered by the sample over the entire measurement range after the background subtraction. Moreover, using Scherrer's formula, the dimensions of crystallites, L_{hkl} ,were calculated in the direction perpendicular to the family of lattice planes (110). These planes give rise to the strongest peak on the diffractogram, located at the scattering angle 2θ ≈ 16.5°.

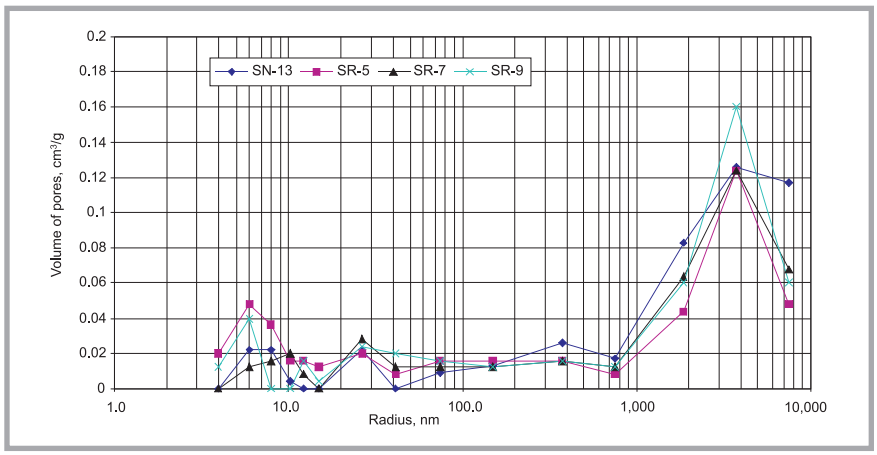

Figure 5. *Size distribution of pores of the fibres after two stage drawing process.*

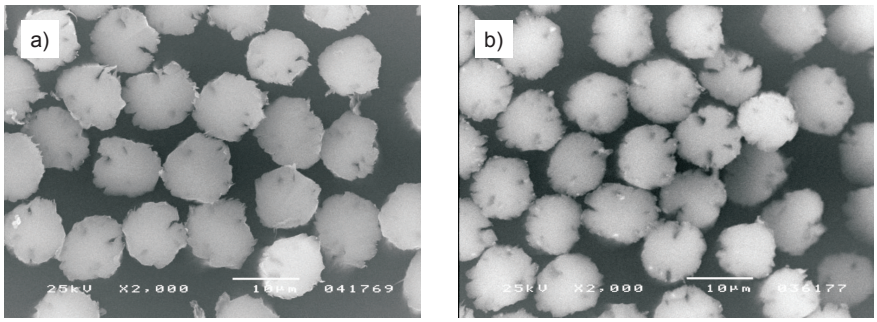

Figure 6. *Photograph of the fibres not containing nanoadditive; a) Cross-sections of the fibres after a two-stage stretching process – SN 13, b) Cross-sections of the fibres after a three-stage stretching process – SN 13/1.*

Results and discussion

In the conditions selected for the solidification process, the strength properties of PAN fibres containing various types of carbon nanotubes are dependent chiefly on the deformation achievable at each stage of the drawing process. This issue is analysed in detail in our earlier work [22]. This work is related to the determination of the effect of the type of nanotube on the deformability and strength properties of fibres obtained with the addition of such tubes. We attempted to obtain total deformation values as high as possible, which was assisted by applying mild conditions at the solidification stage and carrying out the process with a high positive value of the as-spun draw ratio. The aim of this research was to obtain fibres with increased strength properties and with a diameter close to that of microfibres. The use of a positive as-spun draw ratio is advantageous because of the axial orientation of structural elements in the still liquid stream. The degree of orientation is dependent on the value of the lengthwise gradient of the velocity, which varies along the forming route. The associated ordering and parallelising of chains of macromolecules improve the strength properties of the fibres. On the other hand, the use of positive values of the as-spun draw ratio is typically associated with the production of PAN fibres with increased porosity [24], resulting in structural defects, which are not desirable in the case of fibres meant for carbonisation. The presence of carbon nanotubes in the solidifying stream of the spinning solution (as was found in our earlier work) diminishes that effect [22]. This ought to have a positive influence on the properties of the precursor fibres and the carbon fibres obtained from them.

Analysis of the porous structure

In view of the specific features of measurement of the total pore volume by the mercury porosimetry method, it was decided to divide the results of measurement into two values:

- The value of the pore volume corresponding to pores with a radius in the range 3 - 1000 nm. We ascribed this range to the porosity of elementary fibres.
- Total pore volume for the test sample (range: 3 - 7500 nm), including the porosity of elementary fibres and that of the fibrous material (e.g. spaces between fibres).

The criterion for such a division was an analysis of the cross-sections of fibres obtained without nanoadditives. These were not found to contain pores with dimensions outside that range. Account was also taken of conclusions relating to the specific features of porosity determination by mercury porosimetry stated in [29], recognising that a porosity above 1000 nm can be associated with the presence of empty spaces between fibres.

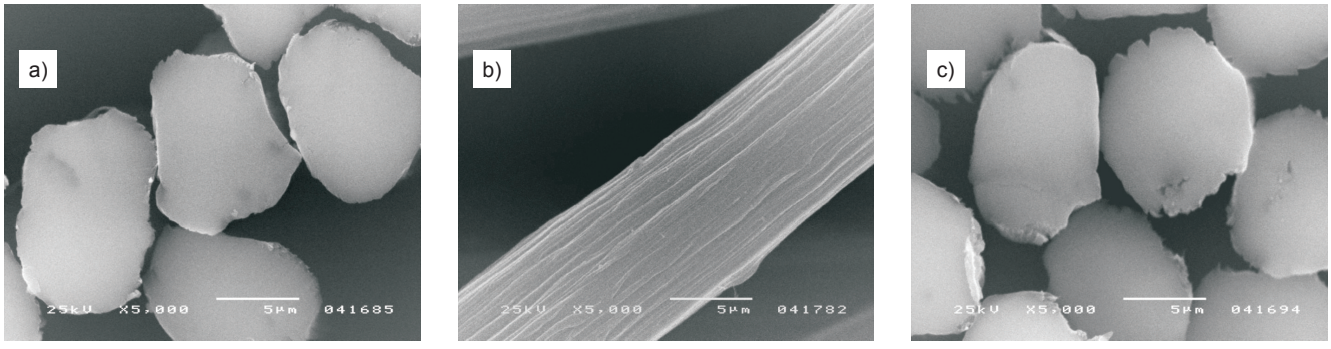

Figure 7. *Photograph of the fibres containing carbon nanotubes; a) Cross-sections of the fibres after a two-stage stretching process – SR 7, b) Lengthwise view of the fibres after a two-stage stretching process – SR 7, c) Cross-section of the fibres after a three-stage stretching process – SR 7/1.*

Analysis of the porous structure of PAN fibres obtained after a two-stage drawing process shows that regardless of the type of nanotubes used and differences in the deformation values achievable, the total volume of pores in the range 3 – 5000 nm in the fibres obtained is contained within the narrow range 0.404 – 0.461 cm^3/g. The total volume of pores in the range 3 – 1000 nm is 0.148 – 0.232 cm^3/g. Also at a similar level is the porosity of the fibres denoted as SN 13, not containing nanotubes (***Table 2***). These values are 0.461 and 0.135 cm^3/g, respectively. There are differences, however, in the internal surfaces of the pores. The lowest internal surface was found for fibres containing MWNT-L, denoted as SR 7, and the highest for those containing single-walled nanotubes, denoted as SR 5. The differences in the internal surface of pores in the fibres analysed correspond to the different heights of the first maximum on the graph of size distribution of pores (***Figure 5***). In the analysis of the internal surface of pores, the values corresponding to the total surface of pores of elementary fibres were not distinguished, as was done in the case of the value for the total pore volume. This was because the value of the internal surface of pores is associated mainly with pores below 100 nm, and the difference between the internal surface of pores in the range 3 – 1000 nm and 3 – 5000 nm is not great, amounting to approximately 0.3 m^2/g.

The size distribution curve also has a high maximum within the range of very large pores. This is probably due to the defects present on the fibre surface in the form of cracks and scratches, which are visible

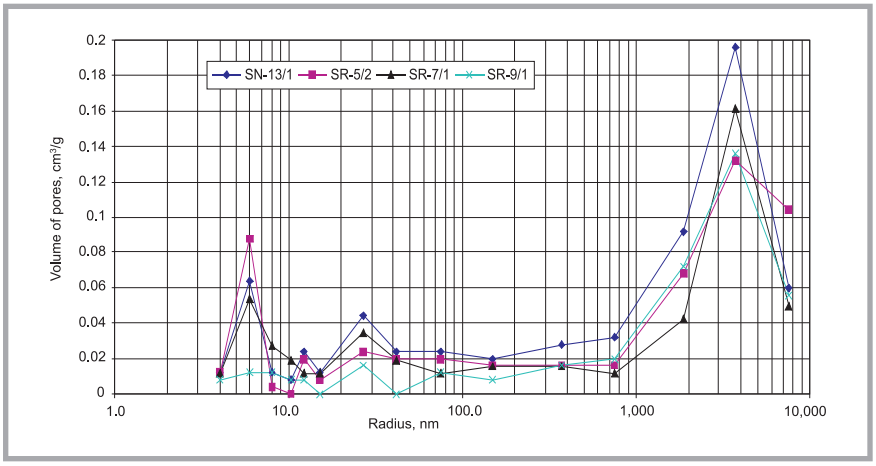

Figure 8. *Size distribution of pores of the fibres after a three-stage drawing process.*

in the lengthwise view of the fibres (***Figure 6***). It also results from empty spaces between elementary fibres of the fibrous material tested.

From the data analysis included in ***Tables 2*** & ***3***, it results that the use of an additional drawing stage led to a change in the value of the total pore volume and in the character of the porous structure of the fibres.

In all cases, with the exception of fibres containing MWNT-S (sample SR 9/1), there was a small increase in the total pore volume, to a level of 0.242 – 0.278 cm^3/g. In the case of fibres without nanoadditives, the total pore volume increased to 0.304 cm^3/g (***Table 2*** and ***3***). The lower values of the total pore volume in the fibres containing nanotubes, compared with fibres without a nanoadditive, indicates the retarding effect of their presence on the processes of mass exchange during solidification, which is confirmed by the scanning microscope photographs of the fibre cross-sections. In the fibres without nanoadditives (***Figure 6***), large pores with a radial orientation are visible. In the fibres with nanotubes, such pores occur sporadically (***Figure 7***). This phenomenon occurs in fibres formed with both two-stage and three-stage drawing processes. During the third stage of drawing, there was a change in the character of the porous structure, in which the volume fraction of small and medium pores increased. The maxima reflecting the proportions of these pores are higher to a degree which depends on the type of nanotubes introduced (***Figure 8***, see page 16). One can also observe an increase in the internal surface of the fibres, except in the case of sample SR 9/1. In the latter case the internal surface decreased by a factor of almost 1.7 compared with sample SR 9. Hence it can be assumed that the

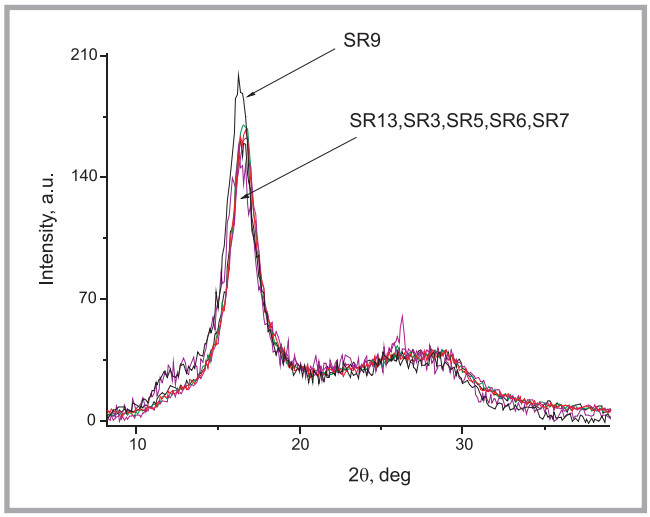

Figure 9. *Diffraction curves of the fibres investigated.*

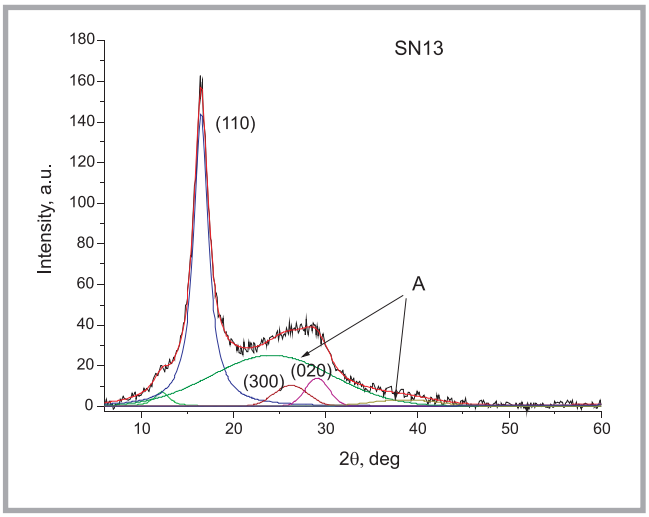

Figure 10. *Resolution of the diffraction curve of sample SN 13 into components.*

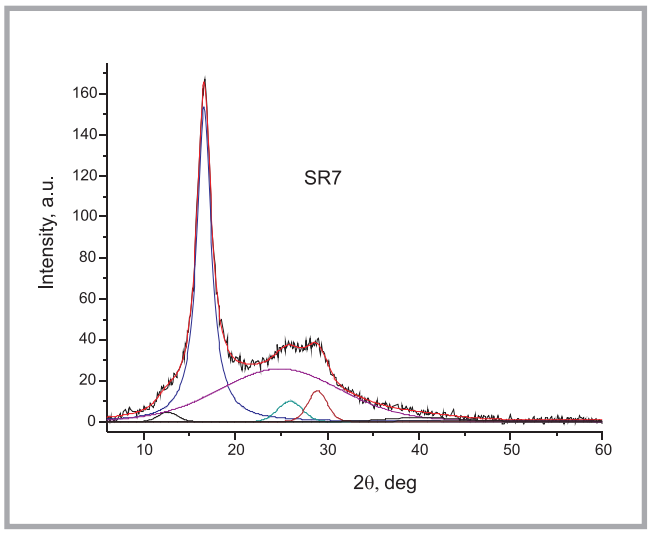

Figure 11. *Resolution of the diffraction curve of sample SR7 into components.*

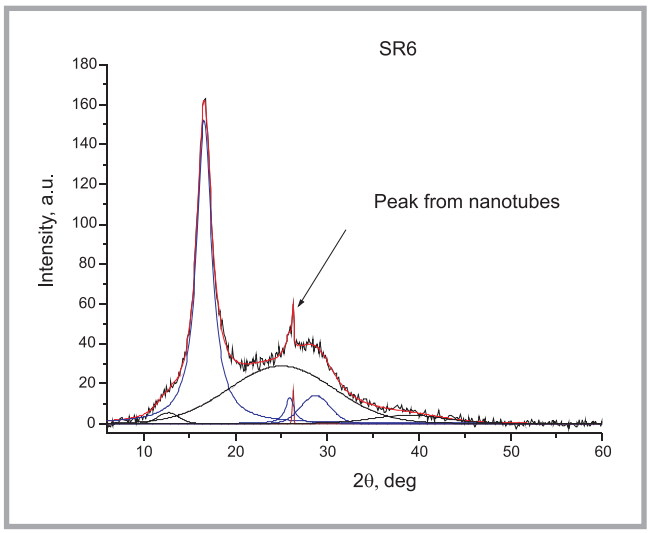

Figure 12. *Resolution of the diffraction curve of sample SR6 into components.*

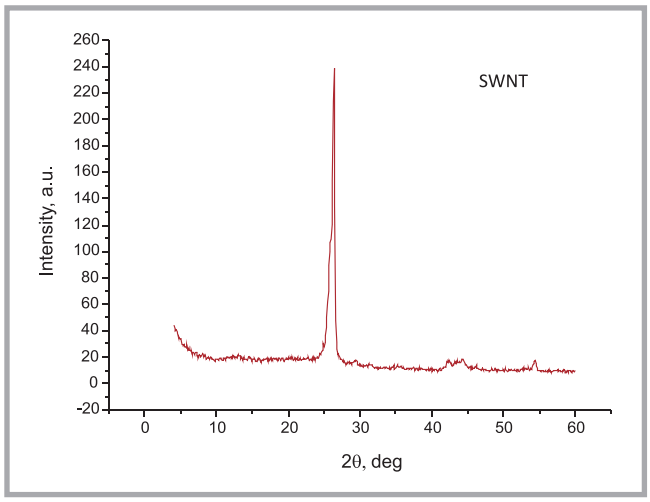

Figure 13. *Diffraction curve of SWNT nanotubes.*

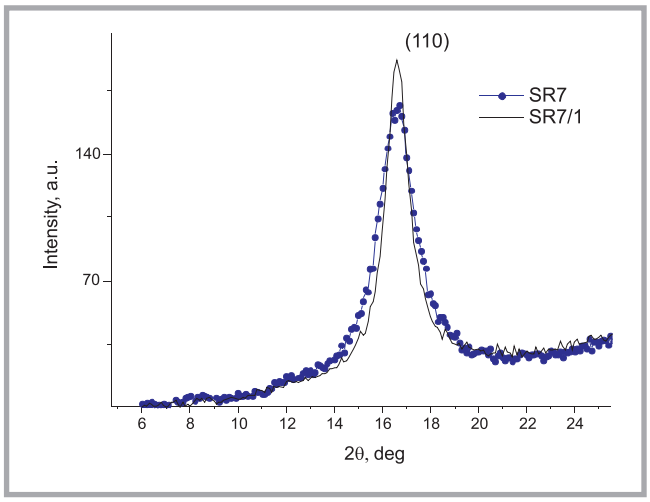

Figure 14. *Diffraction curve of samples SR 7 and SR 7/1.*

highest tenacity in the series for these fibres is also associated with a significantly lower level of defectiveness of the structure. The total pore volume in these fibres fell to 0.120 cm^3/g; the lowest value for any of the fibres considered. Also, during the final drawing stage, there was an alteration in the supramolecular structure of these fibres, which is analysed below. Both these factors – porous and supramolecular structure – determine (alongside the orientation of structural elements) the strength properties of the fibres.

Analysis of the supramolecular structure

A comparative analysis of the supramolecular structure of fibres containing various types of nanotubes with fibres without nanoadditives leads to the following observations: In the case of fibres formed using a two-stage drawing process (***Table 2***), the degree of (para)crystallinity of most of the fibres containing nanotubes is the same as for fibres without nanotubes (SN 13), amounting to c. 55 ± 2 %. The dimensions of crystallites (L_{110}) are also similar. For a direction perpendicular to the lattice planes (110), i.e. perpendicular to the axes of the macromolecules, lying within the range 40–50 Å.

An exception is fibre SR 9, containing MWNT-S with a length of 1 – 2 μm. In this case the degree of (para)crystallinity reaches 68%, but the crystallite dimensions are similar to the others, at ≈ 48 Å. These are the fibres for which the highest values of the total deformation (19.6) and tenacity (570 MPa) were obtained.

The interplanar distance d_{110} is very similar in all crystallites present in the fibres tested, lying in the range 5.3 – 5.4 Å, which indicates an absence of differences in the degree of packing of macromolecules in the crystallites.

Figure 9 shows a set of diffraction curves for all the fibres formed using a two-stage drawing process, after subtraction of the background and normalisation. A significantly greater height of the reflection (110) is clearly visible on the diffractogram of fibres SR 9. The diffraction curves of the other fibres are very similar to each other.

Figure 10 presents a diffraction curve of fibres without nanotubes (SN13) resolved into crystalline peaks and amorphous components. ***Figures 11*** and ***12*** show, for example, diffractograms of fibres SR 7 and SR 6, containing, respectively, 1% and 3% of carbon nanotubes in proportion to the polymer mass. Sample SR 6 was included in the crystallin-

ity measurements due to its higher (3%) proportion of SWNT (these fibres were formed in analogus conditions like the other fibres analysed in this work; properties of fibres: Tenacity 470 MPa, Young's modulus 8.9 GPa, Elongation at break 11.78%, Crystallinity 55%, L110 - 45 Å, d110 – 5,3; properties of fibres after three stage drawing – sample SR 6/1: Tenacity 580 MPa, Young's modulus 11.5 GPa, Elongation at break 9.86%, Crystallinity 51%, L110 - 79 Å, d110 – 5,3). In the case of fibres SR6, there is a small peak clearly visible on the diffraction curve at an angle of $2\theta \approx 26°$, due to the nanotubes. For comparison, ***Figure 13*** shows a diffraction curve for the SWNH nanotubes used in those fibres.

The use of three-stage drawing has a different influence on the degree of crystallinity of the fibres tested. In the case of standard fibres, there is a marked increase in the degree of crystallinity, up to 62% (sample SN 13/1) in comparison with the fibres obtained using two-stage drawing (sample SN 13).

In the case of fibres with nanotubes, there is a decrease in the degree of crystallinity in comparison with fibres obtained from two-stage drawing, although the extent of the decrease varied for different samples. The smallest decrease, around 1%, was recorded for samples containing MWNT-A (SR 3/1). In other fibres, the decrease amounts to 3% and 9% for SWNT with a concentration of 3% (SR 6/1) and 1% (SR 5/2), and 10% and 14 % for MWNT-L and MWNT-S, respectively (SR 7/1 and SR 9/1).

Generally, in the case of fibres obtained using three-stage drawing, the degree of crystallinity of fibres containing nanotubes (SR 3/1, SR 5/2, SR 6/1, SR 7/1 and SR 9/1) is markedly lower than that of fibres without nanoadditives (SN 13/1 – 62%); the highest value was recorded for fibres containing MWNT-A (SR 3/1 – 56 %).

There is, however, a very distinct decrease in the peak (110) width at its half -height (***Figure 14***), which indicates a significant increase in the dimensions of the crystallites compared with fibres obtained after two-stage drawing. In both standard fibres and those containing nanotubes, this dimension exceeds 70 Å, (an increase of almost 70%). The crystallite dimension considered in this analysis is in a direction perpendicular to the axis of the macromolecules. The effect observed is probably associated with the orientation crystallisation. As a result of drawing the fibres, successive macromolecules are straightened, becoming oriented parallel to the axis of the fibres and joining onto the crystallites, which are also oriented parallel to the axis. This leads to an increase in the lateral dimension of the crystallites.

As in the case of fibres obtained by two-stage drawing, the interplanar distance d_{110} in the crystallites is very similar, lying in the range 5.3 – 5.4 Å, which indicates an absence of differences in the degree of packing of macromolecules in the crystallites.

The lower degree of crystallinity of fibres containing carbon nanotubes after the three-stage drawing process than those after two-stage drawing indicates that some of the crystallites (probably the smallest, least perfect and most chaotically arranged) vanish as a result of local stresses which appear in the fibre during the third stage of the drawing process. Probably the presence of nanotubes, which during drawing tend to achieve an orientation parallel to the axis of the fibre, leads to a local concentration of stresses, causing the elimination of the crystals. This disintegration may be encouraged by the increased temperature of this stage of the drawing process and the increased molecular mobility of the macromolecules associated. At the same time, the remaining crystallites – those which are larger and better oriented along the axis of the fibre – grow in a direction perpendicular to the axis as a result of the orientation crystallisation mechanism described above.

The alteration of the porous structure which takes place at successive stages of the drawing process, combined with changes in the degree of (para)crystallinity, probably proceeds in the following way: During the third stage of drawing, the local concentration of stresses may cause disintegration of some of the smaller and less well oriented paracrystalline regions, which leads to the formation of empty spaces (pores) in these regions, with dimensions comparable to those of the regions. As a result, the total pore volume increases, and at the same time the volume fraction of small and medium pores also increases. Such an increase may also be due to a change in the shape of larger pores occurring during the drawing process, from spherical to almost ellipsoidal. These can become classified as smaller pores, because in mercury porosimetry it is the smallest lateral dimension of a pore that is taken into account.

It is also known that during the drawing process, the straightening and parallelisation of macromolecules is accompanied by a decrease in the diameter of fibres. An increase in the density of macromolecules and their local, closer packing in unordered regions results, as a rule, in a decrease in the porosity of the fibres. There may also be a decrease in the dimensions of empty spaces between groupings of macromolecules. These spaces determine the porosity of the fibres in the small and medium pore range, also influencing the value of the pore internal surface. In the case of fibres SR 9/1, the latter phenomenon probably dominates those described previously. This may explain a decrease in both the total pore volume and pore internal surface area of these fibres, in comparison with the values obtained after two-stage drawing.

The analysis above leads to the supposition that in the case of fibres SR9, containing MWNT-S, the highest tenacity value obtained after a two-stage drawing process is associated with their internal structure, created thanks to their high deformability. Probably the ability to reach deformations of the order of 19.6 is also associated with the positive effect of the presence of a specific type of nanotube (MWNT-S) in the fibre material. With a porosity similar to that of other fibres, this structure has the highest degree of (para)crystallinity, around 68%. As a result of the alteration of this structure during the third drawing stage, the sizes of crystallites increased significantly, accompanied by a decrease in the degree of (para)crystallinity. However, the structure formed has the lowest level of defectiveness, and the total volume of pores in the range 3 – 1000 nm is around 0.120 cm^3/g, which contributes to the highest in the series; the tenacity of these fibres is 630 MPa. A similar level of tenacity, around 620 MPa, is obtained for fibres SR 7/1, which contain MWNT-L. With these, at a lower degree of paracrystallinity (43%) and with similar crystallite sizes, their equally high strength properties are due to a higher deformability in the last stage of drawing (the total deformation value was 23.47, compared with 21.5 for sample SN 9/1, with simi-

lar deformations in two-stage drawing). These differences in deformations are connected with the presence of MWNT-L in the material. In spite of the higher porosity of these fibres, the alteration of the porous structure towards a decrease in pore dimensions was significant (***Figure 5 and 8***). There was an increase in the volume fraction of small and medium pores combined.

At the same time, the fibres with lower tenacity considered (SR 7/1) have a higher Young's modulus by approximately 1.2 GPa than that of fibres with a higher tenacity (SR 9/1), which may be connected with their somewhat greater crystallite dimensions. Such an influence of crystallite dimensions on the Young's modulus for PAN precursor fibres has already been identified in our work [24]. For all the types of nanocomposite fibres where a third stage of drawing was used, the Young's modulus rose by 0.6 GPa, which was highest in the case of fibres containing long multi-walled nanotubes, reaching 3.58 GPa. For the fibres without nanoadditives, the values of Young's modulus after both stages of the process are similar.

It is characteristic that the strength of fibres not containing nanotubes was 90 – 100 MPa lower in comparison with both types of nanocomposite fibres with the best properties, which is probably due to the significantly lower values of total deformation that were achieved for these fibres (around 18.6) and the resulting lower degree of orientation of structural elements.

In the three-stage drawing process, the value of total deformation for these fibres increased only slightly. Although they had a higher degree of paracrystallinity (62%) and similar crystallite dimensions, the level of defectiveness in the macroscopic structure of these fibres was greater, and the total pore volume was significantly higher than in nanocomposite fibres, amounting to 0.3 cm^3/g.

This is understandable because, apart from the orientation of the macromolecules, the strength properties of fibres are determined by all of the parameters of the macroscopic and supramolecular structure, as well as the possibility of secondary bond formation between the macromolecules of the material.

Conclusions

- With a similar level of the defectiveness of the structure (total pore volume 0.15 – 0.20 cm^3/g) and small changes in the dimensions of crystallites, the differences in the tenacity of PAN nanocomposite fibres after a two-stage drawing process are associated mostly with the axial orientation of structural elements. The formation of a structure with a higher degree of (para)crystallinity is favoured by the presence of MWNT-S in the fiber material, which results in higher strength properties of these fibers compared with fibres containing long multi-walled nanotubes and those with single-walled nanotubes.
- The use of three stages of drawing, as in the process of forming PAN fibres modified with carbon nanotubes, causes an alteration in their porous structure, tending towards smaller pore dimensions; however, this is accompanied by an unfavourable increase in the total pore volume. Only in fibres containing short multi-walled nanotubes does a favourable decrease in porosity take place.
- Another result of the use of a three-stage drawing process is the alteration of the supramolecular structure of all types of nanocomposite fibres. One can observe a decrease in the degree of paracrystallinity, accompanied by an increase in the dimensions of crystallites (as a result of orientation crystallisation). This effect is dependent on the type of nanotubes contained in the material of the fibres.
- The presence of carbon nanotubes in the material of the fibres improves their deformability, which is the main reason for their higher strength properties compared with fibres without a nanoadditive.

Refenences

1. *Jonhson W., The structure of PAN based karbon fibers and relationship to physical properties, vol. 1, Amsterdam: North-Holland, 1985.*
2. *Kumar S., Anderson D. P., J. Mater. Sci. 28, 1993, pp. 423-439.*
3. *Mikołajczyk T., Boguń M., Błażewicz M., Piekarczyk I.; Journal of Applied Polymer Science; 100 (2006) pp. 2881-2888.*
4. *Mikołajczyk T.; Boguń M.; Kowalczyk A.; Fibres & Textiles in Eastern Europe 13(3), 2005, pp. 30-34.*
5. *Boguń M., Mikołajczyk T., Kurzak A., Błażewicz M., Rajzer I.; Fibres & Textiles in Eastern Europe, 14(2),2006, pp. 13-16.*
6. *Boguń M., Mikołajczyk T.; Fibres & Textiles in Eastern Europe 14(3), 2006, 19-22.*
7. *Mikołajczyk T., Boguń M., Rabiej S.; Journal of Applied Polymer Science; 105, 2007 pp. 2346-2350.*
8. *Mikołajczyk T., Rabiej S., Boguń M.; Journal of Applied Polymer Science 101, 2006, p. 760.*
9. *Chae H. G., Sreekumar T. V., Uchida T., Kumar S.; Polymer 46 (2005) pp. 10925-10935.*
10. *Sreekumar T. V., Liu T., Min B. G., Guo H., Kumar S., Hauge R. H., Smalley R. E.; Advanced Materials 10 No. 1 (2004) pp. 58-61.*
11. *Chae H. G., Minus M. L. , Kumar S.; Polymer 47 (2006) pp. 3494-3504.*
12. *Ajayan P. M., Schadler L. S., Giannaris C.; Advanced Materials 12 (2002) pp. 750-753*
13. *Jortner J.C., Rao N. R.; Pure Applied Chemistry; 74 (2002) pp. 1491 – 1506.*
14. *Przygocki W., Włochowicz A.; Fulereny i nanorurki, Wyd. Naukowo-Techniczne, Warszawa 2001.*
15. *Dresselhaus M. S., Dresselhaus G., Carbon Nanotubes: Preparation and Properties, CRC Press, New York 1996.*
16. *Mamalis A. G., Vogtlander L. O. G.; Precision Engineering 28 (2004) pp. 16-30.*
17. *Baughman R. H., Zakhidov A .A., Heer W. A.; Science 297 (2002) pp. 787-792.*
18. *Boguń M. ,New Generation Precursor PAN Fibres Containing Ceramic Nanoadditioni' (in Polish). Ph. D. Thesis. Technical University of Lodz, 2007.*
19. *Mikołajczyk T., Janowska G., Wójcik M., Boguń M., Kurzak A.; Journal of Applied Polymer Science 109 (2008) pp. 2513-2521.*
20. *Mikołajczyk T., Boguń M., Kurzak A., Wójcik M., Nowicka K.; Fibres & Textiles in Eastern Europe 15(3), 2007, pp. 19-24.*
21. *T Mikołajczyk., Szparaga G., Janowska G.; Influence of Silver Nano-additive Amount on the Supramolecular Structure, Porosity and Properties of Polyacrylonitrile Precursor Fibers; Polymers for Advanced Technologies; Published online in Wiley InterScience: 2009.*
22. *Mikolajczyk T., Szparaga G., Bogun M., Fraczek-Szczypta A., Błażewicz S.; Effect of spinning conditions on mechanical properties of PAN fibres modified with carbon nanotubes; Journal of Applied Polymer Science; in press.*
23. *Mikołajczyk T.; Fibres & Textiles in Eastern Europe 5 (1), 1997, pp. 42-47.*
24. *Mikołajczyk T.; Modification of the manufacturing proces sof polyacrylonitrile fibres; Scientific Thesis of Technical University of Lodz, No 784, Łódź 1997.*
25. *Rabiej M., Rabiej S.; „Analiza rentgenowskich krzywych dyfrakcyjnych polimerów za pomocą programu komputerowego WAXSFIT" Wydawnictwo ATH, Bielsko-Biała 2006.*
26. *Powell M. J. D., Comput. J., 7 (1964) 155.*
27. *Stefani R., Comp. trend. 251, (1960), p. 2174.*
28. *Brandrup J., Immergut E. H., Grulke E. A., Polymer Handbook, Wiley, New York 1999.*
29. *Nagy V., Laszlo M. Vas; Fibres & Textiles in Eastern Europe, 13(3), 2005, pp. 21-26.*

Received 20.04.2009 Reviewed 27.102009

Kaunas University of Technology (KTU)

Kaunas, Lithuania

The roorts of the university go back to 1920 when the first centre of university-type higher courses was established. In 1922 the Government of Lithuania accepted a resolution establishing Kaunas University, which was then given the name of Vytautas the Magnus in 1930. In 1950 Kaunas University was reorganized into Kaunas Polytechnic Institute (KPI) and Kaunas Medical Institute. In 1990 KPI changed its name to the present name of Kaunas University of Technology (KTU). Now KTU is the largest technological University not only in Lithuania, but also in all the Baltic States. Many Prime Ministers, Ministers, Members of the Lithuanian Parliament and even the President of the Republic of Lithuania have graduated from KTU.

The University is the only one in Lithuania engaged in textile engineering. The Department of Textile Technology dates back to 1929, when the decision to begin education in textile engineering at the University was accepted, and in 1932 the first lectures started. The Department of Textile Technologies, as an organisational unit, was established in 1940, due to the founding of a Laboratory of Fibre Technology in 1936. The creator and first Head of the Department was Professor J. Indriunas. Up to now more than 2500 students have graduated in textile technology (including more than 200 from Latvia and Estonia) and more than 80 postgraduate students have been awarded a Ph. D. degree. The majority of textile engineers of the Lithuanian textile industry graduated from this department. Senior Professors of the Department, such as A. Matukonis, V. Milašius, and A. Vitkauskas are well known not only in Lithuania, but also in Poland and the whole of Europe.

Today the Department's staff includes 7 professors, 4 associate professors, 7 lecturers and 12 doctoral students. Up to now more than 2000 scientific articles have been published in Lithuanian and international journals as well as in conference proceedings. The main fields of research activity carried out by the Department of Textile Technology are as follows:

- *the rheological properties of textiles,*
- *the flammability and heat transfer of textiles,*
- *the wettability of textiles,*
- *computerised structural design,*
- *the development of textile manufacturing technologies, and*
- *the manufacturing of nanofibres, among others.*

The department is a member of the international Association of Universities for Textiles (AUTEX). The Professors of the Department have given lectures at various European universities regarding the activities of AUTEX and the European Masters Studies Programme in Textile Engineering (E-TEAM).

Kaunas University of Technology,
Studentų 56, LT-51424 Kaunas, Lithuania
http://www.textiles.ktu.lt/ E-mail: kat0504@ktu.lt